

Number distributions for fermions and fermionized bosons in periodic potentials

Michael Budde and Klaus Mølmer

*QUANTOP, Danish National Research Foundation Center for Quantum Optics,
Department of Physics and Astronomy, University of Aarhus
DK-8000 Aarhus C, Denmark*

We compute the spatial population statistics for one-dimensional fermi-gases and for bose-gases with hard core repulsions in periodic potentials. We show how the statistics depend on the atomic density in the ground state of the system, and we present calculations for the dynamical turn-on of the potential.

PACS numbers: 03.75.Fi, 42.50.Ct

INTRODUCTION

Since the first achievement of Bose-Einstein condensation (BEC) of alkali gases in 1995, atomic quantum gas research has continued to provide important tests of fundamental physics. One very ambitious current goal for ultra-cold atom research involves cold fermionic atoms, where association of the fermionic atoms into bose condensed diatomic molecules has just been reported by several groups [1], and where current efforts aim at the observation of BCS superfluidity of the gas [2]. Another goal is to push the study of cold bosons far beyond the mean field regime, as exemplified already when bosons with a repulsive interaction are exposed to a periodic potential giving rise to the transition to a Mott insulator [3, 4], and in the case of a very dilute gas in one dimension, where the repulsive interaction effectively presents a hard core exclusion of overlapping atomic population and leads to the Tonks-Girardeau regime [5].

The zero temperature state of the Tonks-Girardeau bose-gas (TG-gas) is described by a wave function which is obtained mathematically from the Slater determinant describing a spin-less non-interacting fermi-gas. This has the consequence that these two systems have many common properties, and in the present paper we wish to determine one of these properties, namely the fluctuations in the number of atoms populating a finite region of space. The population statistics in weakly interacting and in ideal dilute Bose gases was studied in [6, 7], which revealed a pair-correlation mechanism for finite numbers of non-condensed particles. Measurements of fluctuations represent an interesting approach to the analysis and understanding of physical systems which, in analogy with pioneering experiments in quantum optics, extracts its information from the noise rather than from mean values in measurements. In other many-body problems, noise measurements have already been used to demonstrate the fractional quantum Hall effect, and the Hanbury-Brown and Twiss correlations in high energy nuclear collision experiments where they may constitute probes of quark-gluon plasma effects.

We note that a TG-gas recently was produced and ob-

served in experiments, where a periodic potential was used to alter the effective mass and hence the importance of the interaction energy relative to the kinetic energy of the particles [8]. The analysis in that paper was based on measurements of the momentum distribution. In this paper we develop the theory for another observable of this system, namely the counting noise in real space. We shall also subject our atoms to periodic potentials and investigate how this alters the counting statistics.

SPATIAL POPULATION STATISTICS FOR FERMIONS AND TG-BOSONS

A pure state of N non-interacting spin-polarized fermionic particles (i.e., all populating the same internal spin state) is described by an anti-symmetrized product state (Slater determinant) of single-particle spatial wave functions

$$\Psi_F(x_1, \dots, x_N) \propto \det\{u_i(x_j, t)\}, \quad (1)$$

where the N orthogonal single-particle states $u_i(x, t)$ are all solutions of the single-particle Schrödinger equation of the atoms. The stationary ground state is thus obtained from the N lowest single-particle energy eigenstates.

A pure state $\Psi_B(x_1, \dots, x_N)$ of N impenetrable bosons must be symmetric under exchange of the atomic coordinates, and it must satisfy the condition that it vanishes if any two particle coordinates coincide: $\Psi_B = 0$ if $x_i = x_j$ for any $i \neq j$. In the limit where the hard-core interaction between the boson has zero range, a state vector $\Psi_B(x_1, \dots, x_N)$ obeying these constraints is formally obtained by introducing the antisymmetric function $A(x_1, \dots, x_N) = \prod_{1 \leq i < j \leq N} \text{sgn}(x_j - x_i)$, and simply defining,

$$\Psi_B(x_1, \dots, x_N) = A(x_1, \dots, x_N) \Psi_F(x_1, \dots, x_N). \quad (2)$$

This 'fermionization' ansatz is valid both for stationary states (e.g., the ground state of the system), and for time dependent problems.

When the state vector is known, the probability that precisely n particles are found in an interval of space I , is obtained by an integration over all configurations contributing precisely to this possibility, i.e., n coordinates should be within the interval I and the remaining $N - n$ coordinates should be outside that interval:

$$p(n) = \sum \int_{x_{i_1}, \dots, x_{i_n} \in I} \int_{x_{j_1}, \dots, x_{j_{N-n}} \notin I} dx_1 \dots dx_N \times |\Psi_{F/B}(x_1, \dots, x_N)|^2. \quad (3)$$

The sum extends over all combinations $1 \leq i_1 < i_2 \dots < i_n \leq N$, $1 \leq j_1 < \dots < j_{N-n} \leq N$ with $\forall k, l : i_k \neq j_l$, and although the different contributions to this sum all yield the same value, one still has to carry out an N -dimensional integral of a Slater determinant with $N!$ terms to obtain the distribution. We have written the expression (3) here because it shows explicitly that non-interacting fermions and hard-core interacting bosons have identical number distribution on a given position range. By writing the counting distribution in terms of atomic creation and annihilation operators, we shall obtain a simpler expression for the counting statistics.

The treatment below will address the fermionic system and it will make use of operators with fermionic anti-commutator properties, but the resulting number distributions on spatial intervals are applicable to both non-interacting fermions and impenetrable bosons. Note that the state vectors in momentum space are not linked as easily as the expressions (1,2) in position space: the free fermi gas at zero temperature has a flat momentum distribution up to the fermi momentum, whereas the Tonks gas has a characteristic peaked distribution around zero momentum. In (1) no single-particle state is populated by more than a single atom, whereas the Tonks gas has a single state populated by of the order \sqrt{N} atoms.

Let \hat{a}_n denote annihilation operators for fermions in a state with single-particle wave function $u_n(x)$. The connection between these operators and the position dependent particle annihilation operator $\hat{\psi}(x)$ is

$$\hat{\psi}(x) = \sum_n u_n(x) \hat{a}_n, \quad \hat{a}_n = \int dx u_n^*(x) \hat{\psi}(x) \quad (4)$$

where we make use of both orthogonality and completeness of the basis of eigenstates $u_n(x)$.

In the calculations below, we shall assume that the single-particle states $n = 1, \dots, N$ are all occupied. The probability to detect a single atom at the location x_1 is the expectation value of the local density operator $\hat{\psi}^\dagger(x_1)\hat{\psi}(x_1)$, and we can evaluate the average population of a position interval I as the mean value of the

number operator $\hat{n}_I = \int_{x_1 \in I} dx_1 \hat{\psi}^\dagger(x_1)\hat{\psi}(x_1)$,

$$\langle \hat{n}_I \rangle = \sum_{n'=1}^N \int_{x_1 \in I} dx_1 |u_{n'}(x_1)|^2. \quad (5)$$

Making use of the anti-commutator $\hat{\psi}(x)\hat{\psi}^\dagger(x') + \hat{\psi}^\dagger(x')\hat{\psi}(x) = \delta(x - x')$ we can also address higher order moments of this population,

$$\begin{aligned} \langle \hat{n}_I^2 \rangle &= \sum_{n'=1}^N \int_{x_1 \in I} dx_1 |u_{n'}(x_1)|^2 \\ &+ \sum_{n'=1}^N \sum_{n''=1}^{n'-1} \int_{x_1 \in I} dx_1 \int_{x_2 \in I} dx_2 \\ &\times |u_{n'}(x_1)u_{n''}(x_2) - u_{n''}(x_2)u_{n'}(x_1)|^2. \quad (6) \end{aligned}$$

If we know the single-particle states occupied by the system, we can compute the mean population and the variance in the interval I explicitly. For example, in the lowest energy state of free atoms, where all the eigenstates are plane waves, we obtain for the number of fermions/TG-bosons on a 1D interval of length L : $\langle \hat{n}_I \rangle = \rho L$, where ρ is the mean density of the gas, and we straightforwardly obtain a variance that scales with the logarithm of the mean occupancy of the interval. For an infinitely extended system, one can also obtain this result from the Fermi-Dirac momentum distribution function, which is the Fourier transform of the spatial density-density correlation function [9], $\text{Var}(n_I) = (1 + \ln(2\pi\rho L) + \gamma)/\pi^2$, with Euler's $\gamma = 0.57721\dots$. In quantum optics language, the fermions and TG-bosons are strongly anti-bunched.

Full number distribution

By use of a technique developed by Levitov [10] (for a simpler derivation of this single aspect of Levitov's results, see the presentations by Klich [11] and by Castin [9, 12]), it is possible to obtain the full number distribution $p(n)$ for the number of atoms in the interval I , from which all moments of the distribution are readily calculated. First, we observe that the operator $\frac{1}{2\pi} \int_0^{2\pi} d\theta \exp(i\theta(\hat{n}_I - n))$ is the projection operator onto a subspace where the operator \hat{n}_I has the eigenvalue n , see also [6]. It is therefore useful to introduce the characteristic function

$$F(\theta) \equiv \langle \exp(i\theta\hat{n}_I) \rangle, \quad (7)$$

from which the number distribution is obtained as a simple Fourier transform. The expectation value in (7) is taken in the state with N occupied single-particle wave

functions, and the trick is to realize that this state is described by a density matrix that can formally be written as a thermal state $\sigma = \exp(-\beta\hat{H})/Z$ where $\beta = 1/k_B T$, and where $\hat{H} = \sum \epsilon_n \hat{a}_n^\dagger \hat{a}_n$ is the many-body (second-quantized) Hamiltonian corresponding to a one-body Hamiltonian H (for clarity we write operators acting on the one-particle Hilbert space without hats), which is diagonal in the basis of states $u_n(x)$. The expectation value in (7) is thus the trace of a product of two exponentials of quadratic forms in field creation and annihilation operators. In general, if operators A , B and C on the one-particle Hilbert space obey $\exp(A)\exp(B) = \exp(C)$, then also the relation $\exp(\hat{A})\exp(\hat{B}) = \exp(\hat{C})$ is valid for the second-quantized expressions $\hat{X} = \sum X_{nm} \hat{a}_n^\dagger \hat{a}_m$, $X = A, B, C$. Apart from the factor $1/Z$, our characteristic function is thus the trace of an operator $\exp(\hat{C}) = \exp(\sum_i \lambda_i \hat{b}_i^\dagger \hat{b}_i)$, where λ_i are the eigenvalues of the matrix C , and \hat{b}_i are the corresponding linear combinations of the operators \hat{a}_n . Since the $\hat{b}_i^\dagger \hat{b}_i$ operators are Fermi number operators, their eigenvalues are restricted to the values zero and unity, and the exponential $\exp(\lambda_i \hat{b}_i^\dagger \hat{b}_i)$ yields the values 1 and $\exp(\lambda_i)$. Hence we can write

$$\begin{aligned} \text{Tr}[e^{\hat{A}} e^{\hat{B}}] &= \text{Tr}[e^{\hat{C}}] & (8) \\ &= \text{Tr}[\exp(\sum_i \lambda_i \hat{b}_i^\dagger \hat{b}_i)] \\ &= \text{Tr}[\prod_i \exp(\lambda_i \hat{b}_i^\dagger \hat{b}_i)] \\ &= \prod_i (1 + e^{\lambda_i}) \\ &= \det[1 + e^C] \\ &= \det[1 + e^{A} e^B] \end{aligned}$$

expressing the trace of exponentials of second-quantized operators in terms of a determinant involving exponentials of one particle operators [11]. We now insert the relevant matrices,

$$F(\theta) = \text{Tr}[e^{i\hat{n}_I \theta} \frac{1}{Z} e^{-\beta\hat{H}}] = \frac{1}{Z} \det[1 + e^{i\theta P_I} e^{-\beta H}], \quad (9)$$

where $P_I = \int_{x \in I} |x\rangle\langle x|$ is a projection operator ($P_I^2 = P_I$), and thus obeys $e^{i\theta P_I} = 1 + (e^{i\theta} - 1)P_I$. Introducing the population of the single-particle states, π_n , the characteristic function then rewrites $F(\theta) = \det[1 + (e^{i\theta} - 1)P_I \sum_n \pi_n |n\rangle\langle n|]$, and if we represent this operator as a matrix in a discrete position representation with grid spacing Δx , so that the projection P_I effectively extracts only a sub-matrix with $x, x' \in I$, we get

$$F(\theta) = \det[1 + (e^{i\theta} - 1)\Delta x \sum_n \pi_n u_n^*(x) u_n(x')]. \quad (10)$$

Knowing the single-particle states, either analytically, by diagonalization or by propagation of the time-dependent

Schrödinger equation, this expression allows us to determine the population statistics. As stated above, the expression is valid both for non-interacting fermions and for TG-bosons at zero temperature, where most of our calculations are performed. In this case, $\pi_n = 1$ for all occupied states. We shall also study how the statistics depends on temperature. However, because the Bose-Fermi mapping only holds for $T = 0$, these results only apply to fermions.

Since the determinant is formally a linear combination of products of N_x matrix elements, where N_x is the number of x -values used to represent the interval I , $F(\theta)$ becomes a polynomial in $e^{i\theta}$ of order N_x . This number should be large enough to resolve the spatial structure of the wave functions populated, and we see that the Fourier transform assigns vanishing probability to any number of particles larger than N_x , which is meaningful when we represent the interval by N_x localized basis states. For weakly interacting bosons, their commutators lead to a generating function which has the $e^{i\theta}$ dependence in the denominator [7, 11], and hence any high occupancy is in principle possible. In our numerical calculations, we shall of course check the convergence of our results when larger and larger N_x values are applied.

For comparison, we note that the number distribution of a pure condensate of non-interacting bosons is binomial, i.e.

$$p(n) = \frac{N!}{n!(N-n)!} p^n (1-p)^{N-n}, \quad (11)$$

where $p = \int_{x \in I} dx |u_0|^2$ is the probability for a particular particle to be in I , as given by the macroscopically populated single-particle wave function u_0 in the condensate. This result holds irrespective of the external potential, and in particular, we note that the number distribution for a single lattice site is independent of the amplitude of the periodic potential. This ideal bosonic behavior does not apply when the bosons interact. In the case of repulsive interactions the condensate exhibits a phase transition to a Mott-insulator with a specific number of particles pr. lattice site when the lattice amplitude is raised above a certain value [3, 4].

PARTICLES IN A PERIODIC POTENTIAL: NUMERICAL RESULTS

We shall now use the theory for the spatial statistics to calculate the number distribution of fermions and TG-bosons in a single well of a periodic potential.

Statistics of the ground state

We first investigate the ground state properties of the system, i.e. we assume that the N particles occupy the N

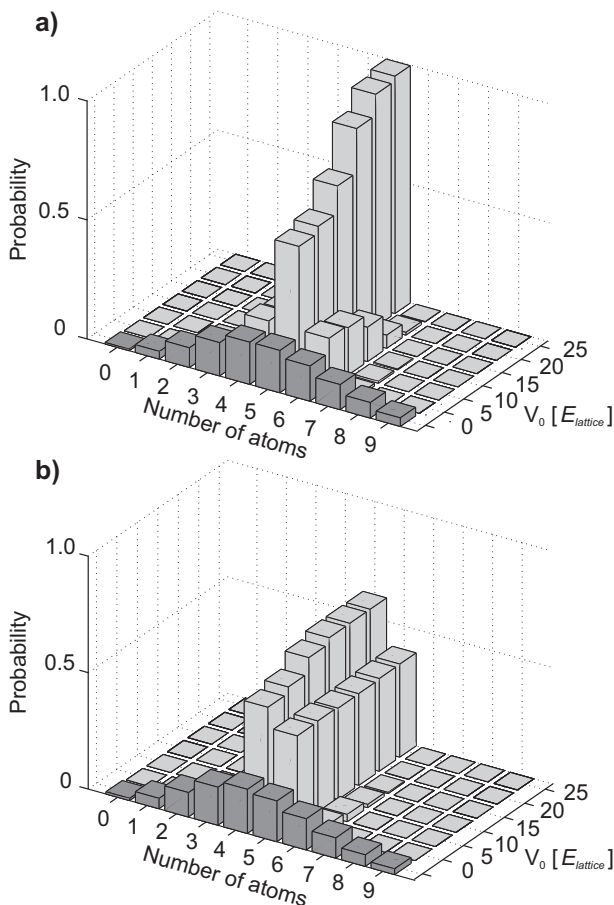


FIG. 1: Atom number distributions for fermions and TG bosons in a single potential well as a function of the lattice amplitude V_0 . a) mean occupation $\bar{n} = 5$ and b) mean occupation $\bar{n} = 4.4$. The distributions were calculated assuming $T = 0$ and that the periodic potential was turned on adiabatically. The amplitude is given in units of the lattice energy E_{lattice} defined in the text. For comparison, the distributions for non-interacting bosons (dark grey bars) are shown at the same mean occupancies.

single-particle states with lowest energy. To find the wave functions $u_n(x)$ of these states required to obtain the number statistics by Fourier transformation of (10), we perform a band structure calculation to solve the single-particle Schrödinger equation

$$-\frac{\hbar^2}{2m} \frac{d^2 u_{n,q}}{dx^2} + \frac{1}{2} V_0 (1 + \cos[\kappa x]) u_{n,q} = \hbar \omega_{n,q} u_{n,q}. \quad (12)$$

Here, m is the atomic mass, and $\kappa = 4\pi/\lambda$, where λ is the wavelength of the optical lattice beams used to create the periodic potential. V_0 is the amplitude of the periodic potential, which is proportional to the intensity of the lattice beams and therefore adjustable experimentally. The natural unit for the amplitude is the lattice energy $E_{\text{lattice}} = 2\hbar^2/(m\lambda^2)$, which differs from the recoil energy associated with the optical lattice beams by a factor of four. Due to the periodicity of the Hamilto-

nian, the wave functions take the Bloch form $u_{n,q}(x) = \exp(iqx)\phi_{n,q}(x)$, where the integer n is the band index and q is the crystal momentum, which under the assumption of periodic boundary conditions over n_w periods, can take n_w discrete values usually taken to be in the first Brillouin zone: $q = \frac{4\pi}{\lambda} \frac{n_q - n_w/2}{n_w}$, $n_q \in \{1, 2, \dots, n_w\}$ [13]. The function $\phi_{n,q}(x)$ is periodic with a spatial period $\lambda/2$. We expand it on a plane-wave basis set $\phi_{n,q}(x) = \sum_{n_b=1}^{2n_b^{\text{max}}+1} c_{n,n_b}(q) \exp[i\frac{4\pi}{\lambda}x(n_b - n_b^{\text{max}} - 1)]$, and solve the Schrödinger equation by finding the coefficients $c_{n,n_b}(q)$ of the eigenvectors of the Hamiltonian in this basis. Once the eigenvectors are known for sufficiently many q , and as a function of V_0 , the effect of the periodic potential on the number statistics can be calculated by insertion of the wave functions into (10) and by calculating the Fourier transform of $F(\theta)$.

Figure 1 shows the number distribution for fermions and TG-bosons at a lattice site as a function of V_0 for two selected mean occupancies $\bar{n} = 5$ and $\bar{n} = 4.4$. Also shown in the figure are the distributions of non-interacting bosons at the same mean occupancy (dark grey bars). For free particles ($V_0 = 0$), the number distribution of fermions and TG-bosons is already much narrower than that of non-interacting bosons. Moreover, the distribution of TG-bosons and non-interacting fermions changes with V_0 , in contrast to non-interacting bosons. In the case of commensurate filling (\bar{n} integer), the distribution becomes $P(n) = \delta_{n,\bar{n}}$ for large V_0 , and consequently the variance of the atom number goes to zero. This is exactly what one would expect for fermions because the Pauli principle makes it energetically favorable to distribute the particles evenly over the lattice sites. When the filling is incommensurate ($\bar{n} = n_{\text{int}} + \epsilon$, where n_{int} is the integer-part of \bar{n}), the distribution becomes bimodal at large V_0 , with $P(n_{\text{int}}) = (1 - \epsilon)$ and $P(n_{\text{int}} + 1) = \epsilon$. Hence, the variance converges towards the value $\text{Var}_I = \epsilon(1 - \epsilon)$, which is symmetric around $\epsilon = 0.5$ and independent of n_{int} . The dependence of Var_I on V_0 is shown in Fig. 2 for a selection of mean occupancies in the range $3 \leq \bar{n} \leq 4$. In addition to the symmetry of the variance around $\epsilon = 0.5$ mentioned above, the figure shows that the lattice amplitude required for the probability distribution to converge increases with the mean occupation. To address this issue quantitatively, we calculated the amplitude $V_0^{\text{var}=1\%}$ required for the variance to be reduced to 1% of the variance for free particles as a function of \bar{n} for integer \bar{n} . Our findings are listed in Table I, which also compares $V_0^{\text{var}=1\%}$ to the mean energy of the highest occupied band $\langle E \rangle_{\text{band}}$ at a lattice amplitude $V_0^{\text{var}=1\%}$. As one might expect, the lattice amplitude has to be slightly larger than the mean energy of the highest occupied band in order to reduce the variance to the few-% level.

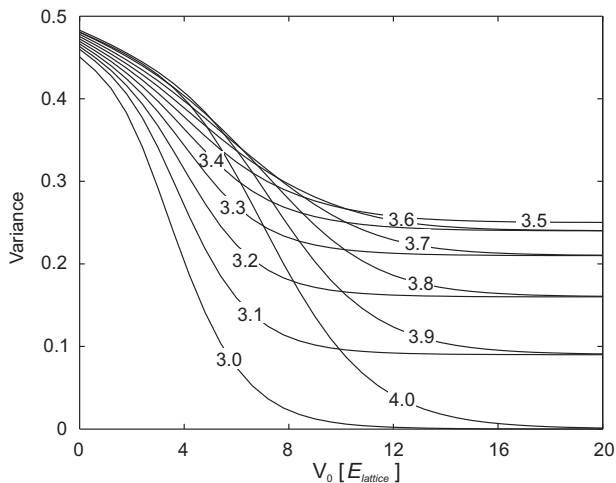


FIG. 2: Variance of the number distribution for fermions and TG-bosons at a single lattice site as a function of lattice amplitude V_0 for various mean occupancies $\bar{n} = n_{int} + \epsilon$. The variance converges towards $\epsilon(1 - \epsilon)$ at large amplitudes. The amplitude required for convergence increases with \bar{n} . The calculations assume that the periodic potential is raised adiabatically and that $T = 0$.

\bar{n}	1	2	3	4	5	6	7	8
$V_0^{\text{var}=1\%} [E_{\text{lattice}}]$	2.5	5.9	10.7	16.8	24.1	32.8	42.7	53.8
$\langle E \rangle_{\text{band}} [E_{\text{lattice}}]$	0.7	3.3	7.2	12.5	19.1	26.9	36.1	46.5

TABLE I: The row $V_0^{\text{var}=1\%}$ lists the lattice amplitude required to reduce the variance of the atom number distribution at a lattice site to 1% of the variance for free particles as a function of the mean occupancy \bar{n} . The row $\langle E \rangle_{\text{band}}$ contains the mean energy of the highest occupied band at a lattice amplitude of $V_0^{\text{var}=1\%}$. The energy unit is E_{lattice} .

Effect of non-adiabatic turn-on

So far we have only considered the ground state of the system, i.e. we have assumed that the periodic potential is turned on *adiabatically*, so that only the N single-particle states with lowest energy are occupied at all times. In reality, the potential will be turned on using a specific ramp $V_0(t)$, and if the ramp is too fast, atoms will be driven into initially unoccupied bands, which will lead to an increase in the atom number fluctuations at a lattice site. We shall now analyze how the lattice turn-on affects the state and the spatial statistics of the many-body system. To this end, we calculate the time-evolution of the state of the system for various ramps by solving the time-dependent Schrödinger equation for the single-particle states.

Our procedure is as follows: At each time t , we expand the single-particle states $\phi_{n,q}^{\text{dyn}}(t)$ on the Bloch eigenfunctions $\phi_{n',q'}^{(0)}[V_0(t)]$ at the amplitude $V_0[t]$ set by the ramp

at that particular time:

$$\phi_{n,q}^{\text{dyn}}(t) = \sum_{n',q'} b_{n,q;n',q'} \phi_{n',q'}^{(0)} e^{-i \int_0^t \omega_{n',q'}(t') dt'} \quad (13)$$

where $\hbar\omega_{n',q'}(t')$ is the energy of the state $\phi_{n',q'}^{(0)}[V_0(t')]$.

This expansion is inserted into the time-dependent Schrödinger equation which results in a set of first-order differential equations for the time dependence of the coefficients $b_{n,q;n',q'}$.

To solve these differential equations, we need to know the matrix elements $\langle \phi_{n',q'}^{(0)} | \frac{d}{dt} \phi_{n'',q''}^{(0)} \rangle$ and the band structure $\omega_{n',q'}$ as a function of $V_0(t)$. We therefore start our calculations by solving the static Schrödinger equation (12) for a sufficiently large number of V_0 's ranging from zero to the final V_0 of the ramp. We then calculate the matrix elements:

$$\langle \phi_{n',q'}^{(0)} | \frac{d}{dt} \phi_{n'',q''}^{(0)} \rangle = \frac{dV_0}{dt} \sum_{n_b=1}^{2n_b^{max}+1} c_{n',n_b}^*(q') \frac{dc_{n'',n_b}(q'')}{dV_0} \delta_{q',q''} \quad (14)$$

Here, $c_{n',n_b}(q')$ are the plane wave expansion coefficients introduced previously. Note that the matrix elements are diagonal in the crystal momentum quantum number and, consequently, the dynamics can be solved for each q independently. Once the matrix-elements and energies of the differential equations have been calculated, the coefficients $b_{n,q;n',q'}$ are propagated in time. We assume that the system is in the ground state initially, i.e. $b_{n,q;n',q'}(t=0) = \delta_{n,n'} \delta_{q,q'}$ for $\{n, q\}$ corresponding to the N states with lowest energy and $b_{n,q;n',q'}(t=0) = 0$ for all other states.

To quantify the degree of excitation caused by the turn-on, the time-evolved single-particle states are used to calculate the population of those Bloch states, which are not populated initially. To make this number independent of the number of periods n_w for the periodic boundary condition, we shall discuss the degree of excitation in terms of the *number of excited atoms pr. period* of the periodic potential N_{exc} . To investigate how the excitations affect the atom number statistics, we also insert the time-evolved single-particle states into (10). There are infinitely many ways to turn on the optical lattice. We shall limit our discussion to two cases: linear and exponential ramps. The linear ramps start at $V_0 = 0$ and increase linearly to the final value $V_{0,\text{final}} = 60E_{\text{lattice}}$ over a time interval of length t_{ramp} . In the experimentally relevant case of ^{40}K fermions and an optical lattice wavelength of $\lambda = 850$ nm, we shall study ramp times up to $80 \hbar/E_{\text{lattice}} \sim 461 \mu\text{s}$. Our exponential ramps have the time-dependence $V_0(t) = V_{0,\text{final}}[\exp(5t/t_{\text{ramp}}) - 1]/[\exp(5) - 1]$, $t \in [0, t_{\text{ramp}}]$. This ramp is very similar to the ones used in the recent experimental realization of a TG-gas [8].

To study the cross-over from nonadiabatic to adiabatic turn-on and the effect on the atom number statistics for a

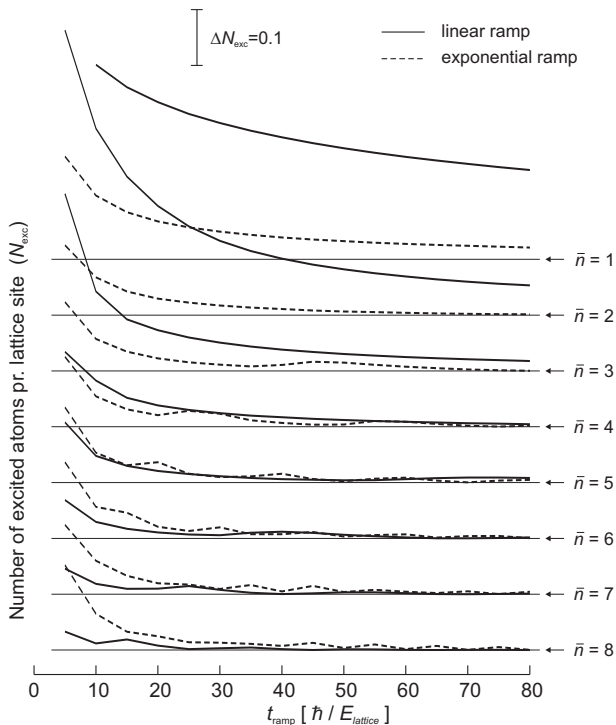


FIG. 3: Number of excited atoms pr. lattice site as a function of the ramp time and of the mean number of atoms pr lattice site (for commensurate filling). The solid (dashed) curves are the results for linear (exponential) time dependencies. For clarity, the curves for different \bar{n} are offset vertically with a spacing of $\Delta N_{\text{exc}} = 0.1$. Thus, the spacing between horizontal lines defines the scale for the vertical axis. The duration of the ramp is given in units of \hbar/E_{lattice} , where E_{lattice} is the lattice energy defined previously. For ^{40}K and an optical lattice wavelength of $\lambda = 850 \text{ nm}$, $\hbar/E_{\text{lattice}} = 5.8\mu\text{s}$

single lattice site, we calculated the time evolution for linear and exponential ramps with durations $5\hbar/E_{\text{lattice}} \leq t_{\text{ramp}} \leq 80\hbar/E_{\text{lattice}}$ and for various mean occupancies \bar{n} . The final amplitude was constant $V_{0,\text{final}} = 60E_{\text{lattice}}$ for all calculations presented here. Fig. 3 shows the number of excited atoms pr lattice site (N_{exc}) as a function of t_{ramp} for integer mean occupancies in the range $1 \leq \bar{n} \leq 8$. The solid curves are the results for linear ramps and the dashed curves represent exponential ramps. The curves corresponding to different \bar{n} are offset vertically from each other by $\Delta N_{\text{exc}} = 0.1$, and for each \bar{n} , the thin horizontal solid line corresponds to $N_{\text{exc}} = 0$. Thus, the spacing between the horizontal lines defines the vertical scale of the figure. Starting in the lower right corner of the figure, we see that for large mean occupancies $\bar{n} \in 7, 8$, and ramp times larger than $\sim 40\hbar/E_{\text{lattice}}$, the number of excited atoms pr lattice site is at or below the few-% level. Thus, the turn-on is essentially adiabatic. Moreover, linear ramps lead to less excitation than the corresponding exponential ramps. This also holds for faster ramps, where the degree of excitation increases. When the mean number of atoms pr site is decreased to

$4 \leq \bar{n} \leq 6$, the excitations caused by the two types of ramps are quite similar. For small mean occupancies, $\bar{n} \leq 3$, exponential ramps are superior because they rise more slowly at early times where the ramp surpasses the energy of the occupied bands.

Our adiabatic calculations show that (cf. Fig. 2) partially occupied bands (incommensurate filling) lead to fluctuations in the number of atoms pr lattice site even at large V_0 . Non-adiabatic turn-on of the periodic potential transfers a fraction of the atoms from the highest occupied to the lowest unoccupied band, and therefore results in (at least) two partially filled bands, which leads to fluctuations in the site occupancy also in the case of commensurate filling. Using the time-evolved single-particle states and our theory for the spatial statistics, we find that the probability distribution at large V_0 for integer \bar{n} broadens compared to the adiabatic monomodal distribution $p(n) = \delta_{n,\bar{n}}$. Except for (a) very fast exponential ramps ($t_{\text{ramp}} \leq 10\hbar/E_{\text{lattice}}$) and (b) ramp durations of $t_{\text{ramp}} \leq 15\hbar/E_{\text{lattice}}$ and small mean occupancies $\bar{n} \leq 2$ for linear ramps, the distribution is to a good approximation given by $\{p(\bar{n}-1) = \eta, p(\bar{n}) = 1-2\eta, p(\bar{n}+1) = \eta\}$, where $\eta = N_{\text{exc}}$. This distribution has a variance of 2η , and the variance can therefore be obtained from Fig. 3 simply by scaling N_{exc} by a factor of two.

Effect of non-zero temperature

All the results presented so far correspond to zero temperature. In this last section we shall discuss how non-zero temperature affects the spatial statistics of fermions in periodic potentials. The bose-fermi mapping (2), which is the reason that the spatial statistics of TG-bosons is identical to that of fermions, does not apply at non-zero temperature. Our theory and the results presented in this section does therefore not apply to TG-bosons.

It is straightforward to generalize our numerical simulations to non-zero temperature. The only difference lies in the occupation probabilities of the states π_n in (10), which for non-zero T are given by the Fermi-Dirac distribution: $\pi_{n,q} = (\exp[\beta(\hbar\omega_{n,q} - \mu)] + 1)^{-1}$, where μ is the chemical potential defined by the constraint that the sum of $\pi_{n,q}$ over all states equals the appropriate total number of particles. We assume that the system is in thermal equilibrium with a temperature T and at the amplitude V_0 , i.e. our results correspond to the case were the system has equilibrated at V_0 . Alternatively one might have assumed that the system equilibrates so slowly that it retains the distribution $\pi_{n,q}$ corresponding to free particles ($V_0 = 0$), and then calculate the statistics using these occupation probabilities. We shall only consider the first case here.

Assuming that the periodic potential has been raised adiabatically, there are two contributions to the fluctu-

ations in the number of particles at a lattice site. In addition to the fluctuations due to the fermionic nature of the particles, which is present at $T = 0$ and was discussed above, thermal excitation lead also lead to fluctuations. This can be seen in Fig. 4, which shows the variance as a function of V_0 for two mean occupancies ($\bar{n} = \{2, 4\}$) and as a function of temperature. The temperature is given in units of E_{lattice}/k_B . In the case of ^{40}K and $\lambda = 850$ nm, the four temperatures are 0 nK, 120 nK, 240 nK, and 360 nK. According to the figure, the variance increases with temperature for a given V_0 due to thermal excitations. For small V_0 , the increase in variance due to thermal excitations decreases when particles are added to the system. The reason is that the mean spacing between bands increases with increasing band index. Since the Fermi-Dirac distribution changes from unity to zero over an energy range $k_B T$, the increase in energy level spacing leads to less thermal excitation. Fig. 4 also shows that the variance, for the case of commensurate filling, goes to zero when the temperature is non-zero. The amplitude V_0 required to obtain a certain variance increases with T . The reason for this behavior is also easily understood. At large V_0 , the particles are localized near the periodic potential minima, and the potential can be expanded to second order around the minima. In this regime the bands are equally spaced with an energy spacing proportional to $\sqrt{V_0}$. Thus, the energy spacing between bands increases with V_0 and, consequently, the thermal fluctuations vanish for large V_0 .

The thermal contribution to the atom number distribution can be studied separately by choosing V_0 such that the variance at $T = 0$ is much less than the variance at the temperature of interest. In this regime, the atom number distribution for commensurate filling is $\{p(\bar{n} - 1) = \eta, p(\bar{n}) = 1 - 2\eta, p(\bar{n} + 1) = \eta\}$, like in the case of excitations caused by non-adiabatic turn-on. In the thermal case, η is equal to $\sum_{n,q} \pi_{n,q}/n_w$, where the sum extends over all the states not occupied at $T = 0$.

CONCLUSION

We have presented a theory for the spatial statistics of fermions and Tonks-Girardeau bosons in one dimension, and applied the theory to the case of fermions and TG-bosons in periodic potentials. The number distribution of fermions and TG-bosons occupying a single lattice site is significantly narrower than that of non-interacting bosons. Moreover, the distribution depends on the amplitude of the periodic potential and becomes bimodal (monomodal for commensurate filling) at amplitudes on the order of the energy of the highest occupied band. This behavior is completely different from that of non-interacting bosons, which is independent of the potential depth.

We also studied the dynamics associated with the turn-

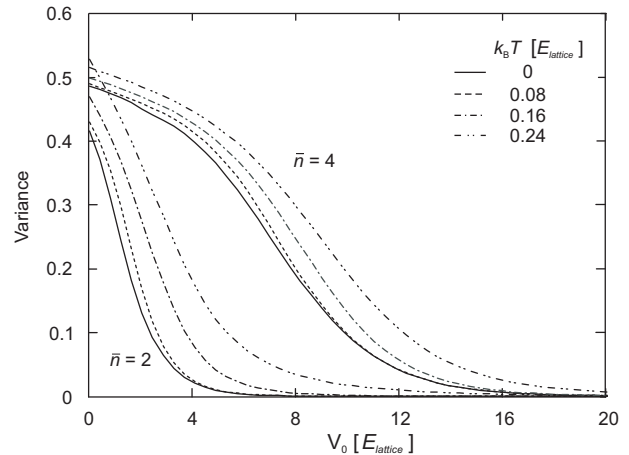


FIG. 4: Variance of the fermion number distribution as a function of V_0 for $\bar{n} = \{2, 4\}$ and temperatures $T = \{0, 0.08, 0.16, 0.24\} E_{\text{lattice}}/k_B$.

on of the periodic potential and the effect of excitations on the number distribution of a lattice site. Non-adiabatic turn-on of the potential leads to partially filled bands and fluctuations in the site occupancy even in the case of commensurate filling. For commensurate filling and most ramps of practical interest, the probability of having one atom more or less than the mean is equal to the average number of excited atoms per lattice site. The variance is well approximated by twice this number.

Finally, we studied how thermal excitations affect the statistics of fermions in periodic potentials. We found that the fluctuations in the number of atoms at a lattice site increase with temperature. The variance of the number distribution converges towards the variance at $T = 0$ when the potential depth is increased, but the potential depth required to obtain a certain variance increases with temperature. For commensurate filling and lattice depths large enough that the fluctuations at $T = 0$ are vanishingly small, thermal excitations lead to a symmetric atom number distribution. Like in the case of non-adiabatic turn-on, the probability of having one atom more or less than the mean is to a good approximation equal to the mean number of excited atoms per lattice site.

Yvan Castin is acknowledged for stimulating discussions and for referring us to the work on the general population statistics.

-
- [1] M. Greiner, C. A. Regal, and D. Jin, *Nature* **426**, 537 (2003); S. Jochim *et al*, *Science* **302**, 2101 (2003); M. W. Zwierlein *et al*, *Phys. Rev. Lett.* **91**, 250401 (2003).
 - [2] C. A. Regal, M. Greiner and D. S. Jin, *Phys. Rev. Lett.* **92**, 040403 (2004); M. W. Zwierlein *et al*, *Phys. Rev. Lett.* **92** 120403 (2004); J. Kinast *et al*, *Phys. Rev. Lett.* **92** 150402 (2004).

- [3] M. P. A. Fisher, P. B. Weichman, G. Grinstein, and D. S. Fisher, Phys. Rev. B **40**, 546 (1989); D. Jaksch, C. Bruder, J. I. Cirac, C. W. Gardiner, and P. Zoller, Phys. Rev. Lett **81**, 3108 (1998).
- [4] M. Greiner, O. Mandel, T. Esslinger, T. W. Hänsch, and I. Bloch, Nature, **415**, 39-44 (2002); M. Greiner, O. Mandel, T. W. Hänsch, and I. Bloch, Nature, **419**, 51-54 (2002).
- [5] M. Girardeau, J. Math. Phys **1**, 516 (1960); E. H. Lieb and W. Liniger, Phys. Rev. **130**, 1605 (1963); A. Lenard, J. Math. Phys **5**, 930 (1964); D. S. Petrov, G. V. Shlyapnikov, and J. T. M. Walraven, Phys. Rev. Lett. **85**, 3745 (2000); V. Dunjko, V. Lorent, and M. Olshanii, Phys. Rev. Lett. **86**, 5413 (2001).
- [6] V. V. Kocharovsky, Vl. V. Kocharovsky, and M. O. Scully, Phys. Rev. Lett. **84**, 2306 (2000).
- [7] I. Carusotto and Y. Castin, Phys. Rev. Lett. **90**, 030401 (2003).
- [8] B. Paredes *et al*, Nature **429**, 277 (2004).
- [9] Y. Castin, private communication.
- [10] L. S. Levitov, H.-W. Lee, and G. B. Lesovik, J. Math. Phys. **37**, 10 (1996).
- [11] I. Klich, cond-mat/0209642.
- [12] Y. Castin, Lectures at Les Houches Center of Physics Workshop, 2003 (to be published).
- [13] N. W. Ashcroft and N. D. Mermin, Solid State Physics (Saunders, 1976).
- [14] At the lattice amplitudes required to reduce the variance to a few percent of the variance at $V_0 = 0$ the bands are essentially flat, i.e. the energies $\hbar\omega_{n,q}$ of a given band are nearly equal.